Supplement of Earth Syst. Dynam., 13, 833–849, 2022
https://doi.org/10.5194/esd-13-833-2022-supplement

Earth System Dynamics
Open Access
EGU

Supplement of

Divergent historical GPP trends among state-of-the-art multi-model simulations and satellite-based products

Ruqi Yang et al.

Correspondence to: Jun Wang (wangjun@nju.edu.cn)

Table S1. Information of the datasets used in this study.

Name	brief description	Reference	Access link
AVHRR NIRv	NDVI and NIRT reflectance from AVHRR	(Wang et al., 2020)	https://figshare.com/s/518a4bdcb14ae95dbcc7
Revised EC-LUE GPP	A new estimation of GPP after adding CO_2 fertilization effect to the generation of EC-LUE model	(Zheng et al., 2020)	**https://figshare.com/articles/dataset/Improved_estimate_of_global_gross_primary_production**
GLASS GPP	Global gridded GPP dataset	(Yuan et al., 2010)	http://www.glass.umd.edu/GPP/AVHRR/GLASS_GPP_005D_YEAR/
FLUXCOM GPP	Global GPP data upscaled based on the FLUXNET eddy-covariance tower measurements	(Jung et al., 2020)	https://www.bgc-jena.mpg.de/geodb/projects/Data.php
FLUXNET2015	Annual GPP observations (GPP_DT_VUT_REF) from 41 flux sites	(Pastorello et al., 2020)	http://fluxnet.fluxdata.org/data/fluxnet2015-dataset/
TRENDY v6 model simulations	GPP and LAI data from ten biome process-based models	(Sitch et al., 2015)	sftp trendy-v6@trendy.ex.ac.uk
GLASS LAI	Global gridded LAI dataset	(Xiao et al., 2016)	http://www.glass.umd.edu/05D/LAI/AVHRR/
CRU v4.0.1	Global gridded temperature and precipitation product based on weather stations	(Harris et al., 2014)	http://data.ceda.ac.uk/badc/cru/data/cru_ts/cru_ts_4.01/

Table S2: Additional FLUXNET sites used. The vegetation types include evergreen needleleaf forest (ENF), croplands (CRO), grassland (GRA), and mixed forest (MF), evergreen broadleaf forest (EBF) and woody savannas (WSA).

Site name	latitude	longitude	Vegetation type	Study period
IT-Lav	45.96°N	11.28°E	ENF	2003–2014
FI-Sod	67.36°N	26.64°E	ENF	2001-2014
FR-LBr	44.71°N	0.77°W	ENF	1996-2008
US-Me2	44.45°N	121.56°W	ENF	2002-2014
CA-TP3	42.71°N	80.35°W	ENF	2003-2014
CA-TP1	42.66°N	80.56°W	ENF	2003-2014
CA-TP4	42.71°N	80.36°W	ENF	2002-2014
CA-Obs	53.99°N	105.12°W	ENF	1999-2010
IT-SRo	43.73°N	10.28°E	ENF	1999-2012
DE-Geb	51.10°N	10.91°E	CRO	2001-2014
US-Ne3	41.18°N	96.44°W	CRO	2001-2013
US-Ne1	41.17°N	96.48°W	CRO	2001-2013
US-Ne2	41.16°N	96.47°W	CRO	2001-2013
DE-Hai	51.08°N	10.45°E	DBF	2000-2012
US-WCr	45.81°N	90.08°W	DBF	1999-2014
ZA-Kru	25.02°S	31.50°E	SAV	2000-2013
RU-Sam	72.37°N	126.50°E	GRA	2002-2014
CA-Gro	48.22°N	82.16°W	MF	2003-2014
AU-Tum	35.66°S	148.15°E	EBF	2001-2014
AU-How	12.49°S	131.15°E	WSA	2001-2014
US-Ton	38.43°N	120.97°W	WSA	2001-2014

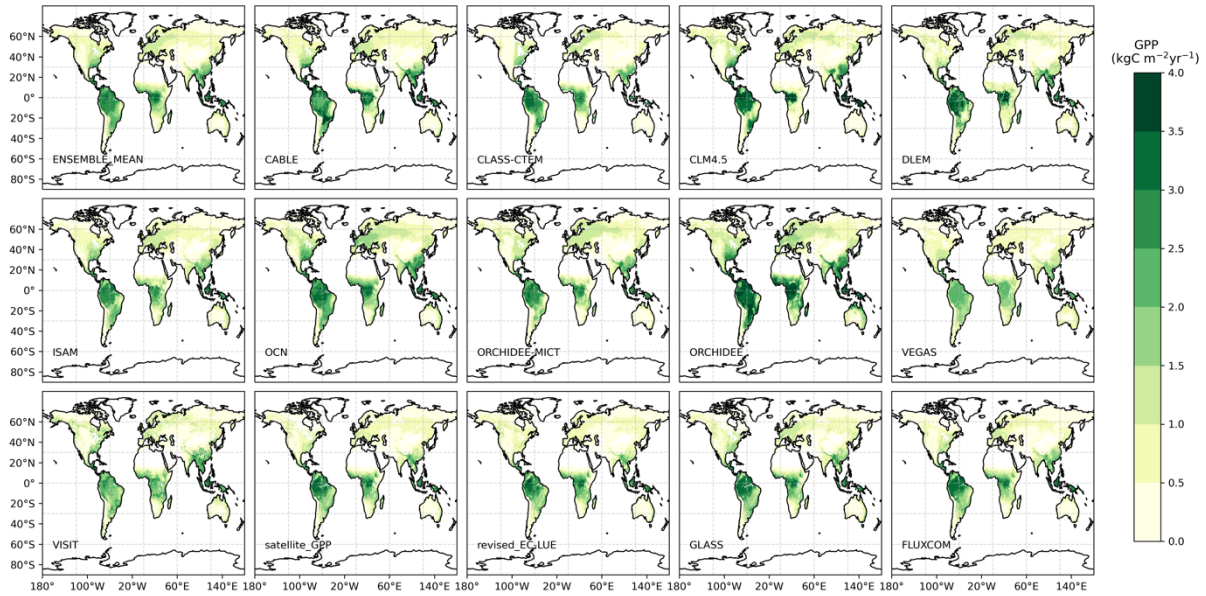

Figure S1: Geographical distributions of climatological annual terrestrial ecosystems gross primary productivity (GPP) from TRENDY DGVM simulations and GPP products (1982–2015). The unit of GPP is kgC m^{-2} yr^{-1}.

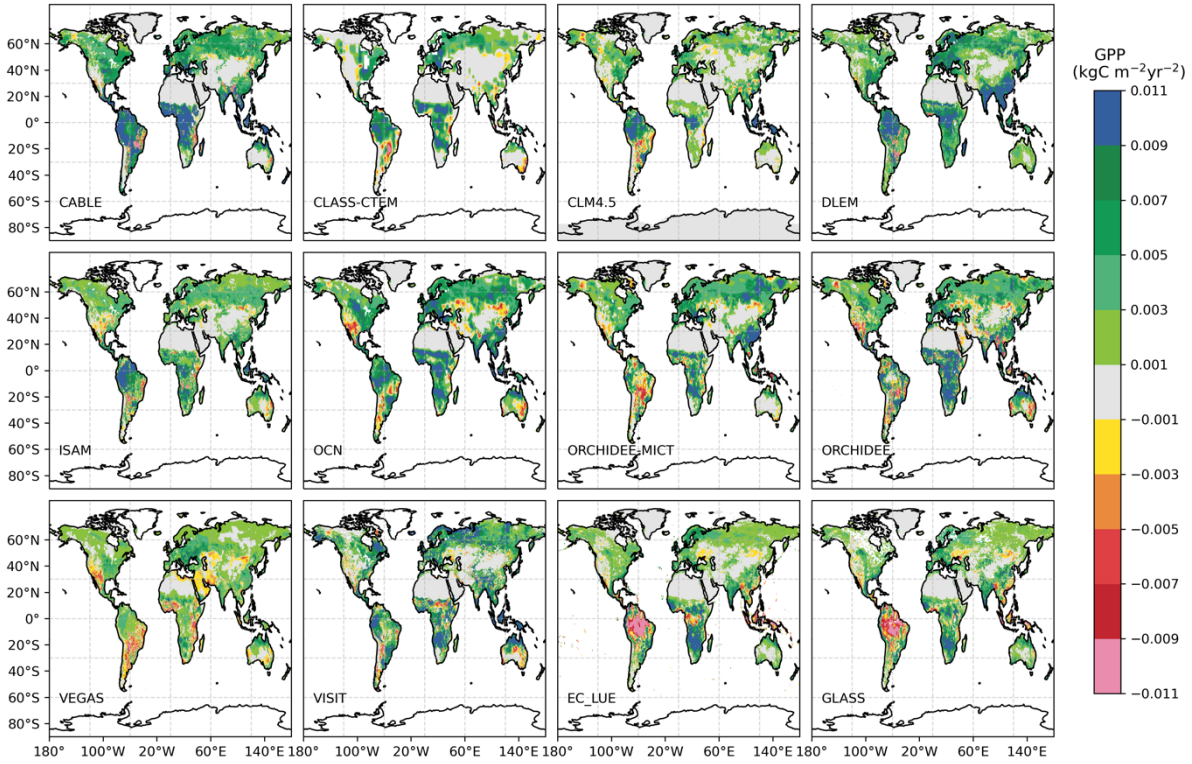

15 **Figure S2. Geographical distributions of linear trends of annual GPP from TRENDY DGVMs and satellite-based products (1982–2015). The unit of GPP trend is kgC m^{-2} yr^{-2}.**

20

25

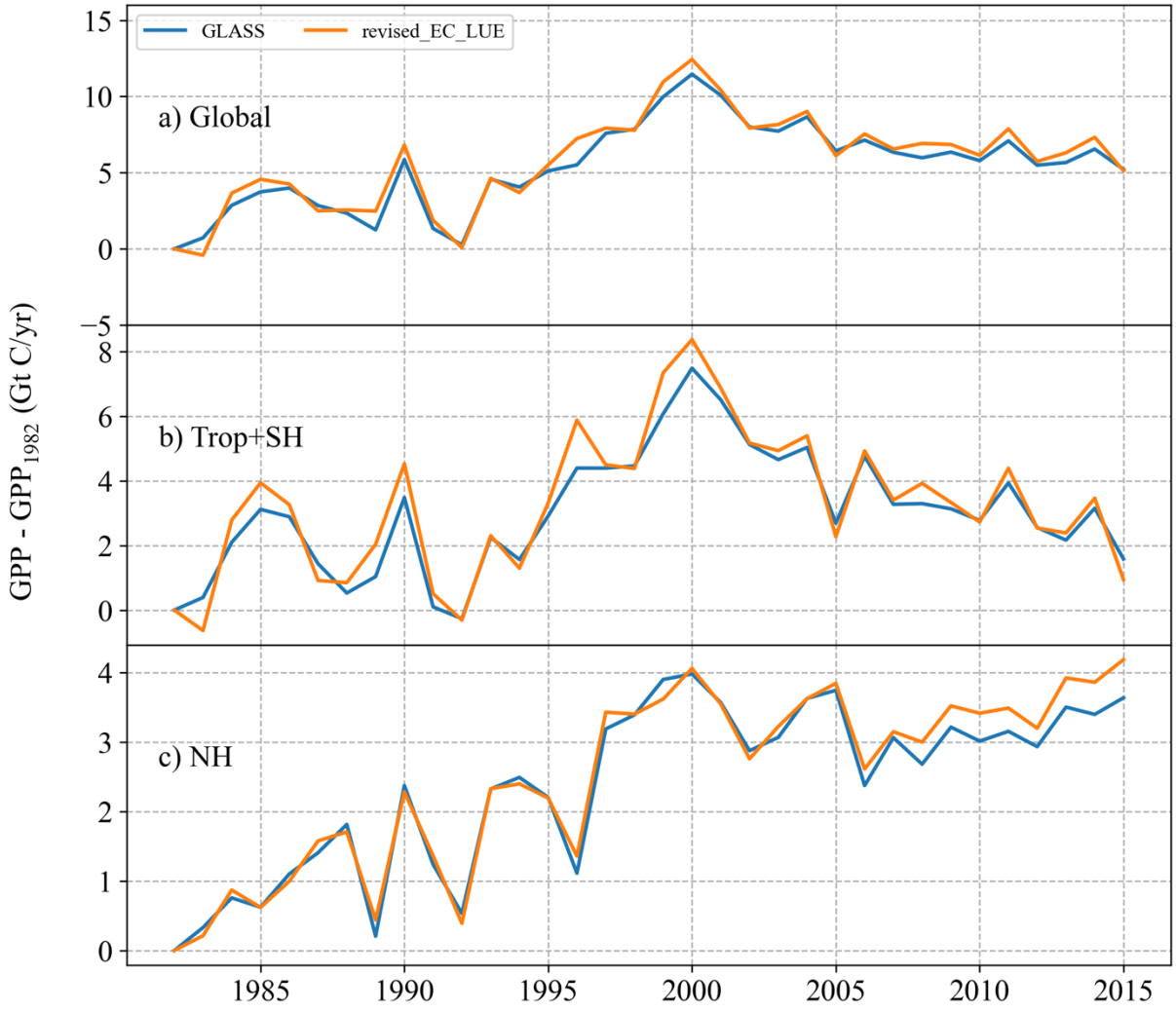

30

Figure S3: Changes of annual total GPP relative to 1982 for GLASS GPP (blue) and revised EC-LUE GPP (orange).

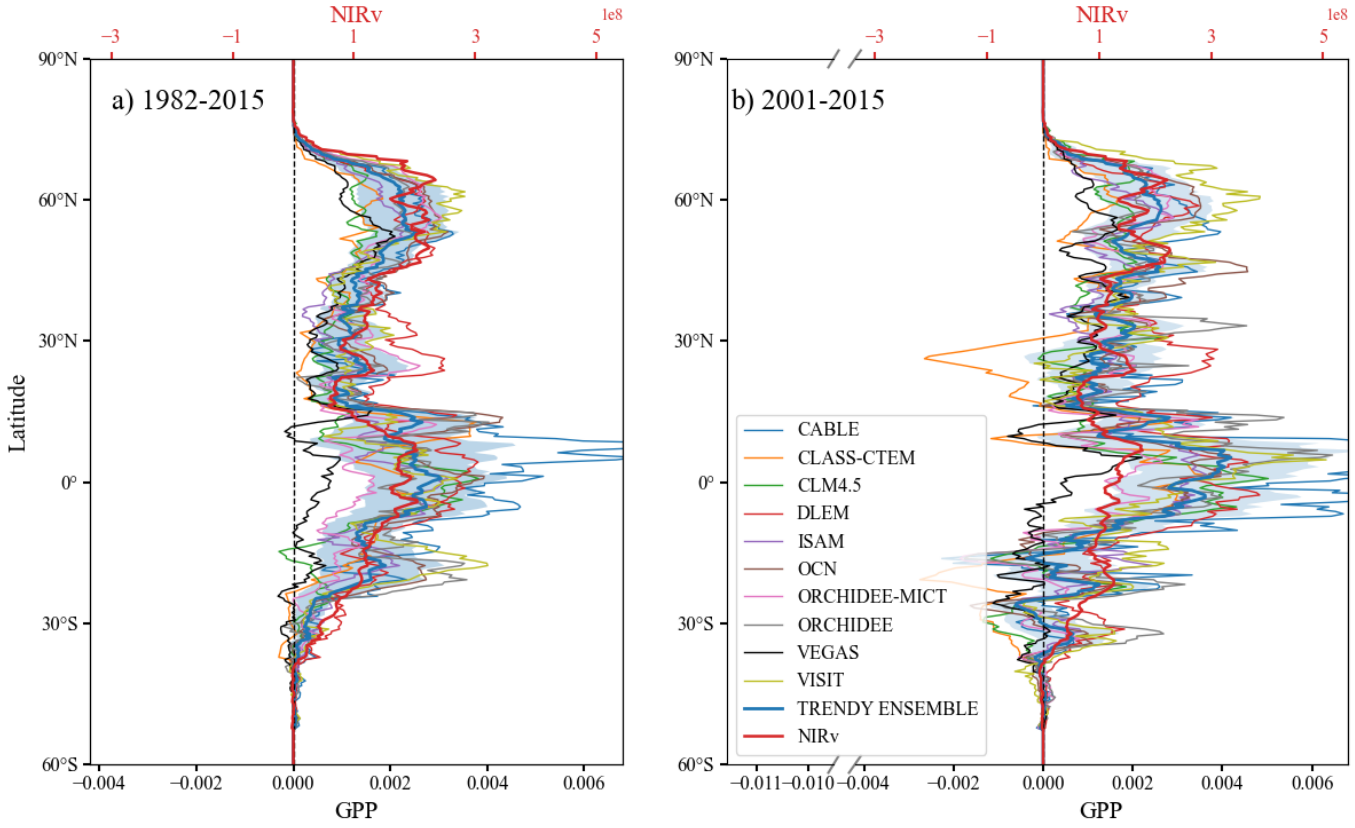

Figure S4: Latitudinal profiles of trends of zonal total NIRv and annual GPP (0.5° latitudinal intervals). DGVM ensemble mean (blue), individual TRENDY model simulations (grey), and NIRv (red) during 1982–2015 (a) and 2001–2015 (b), respectively. The shaded areas represent the standard deviation of the individual TRENDY model simulated GPP trend. The trends of NIRv and GPP are unitless and GtC yr^{-2}, respectively.

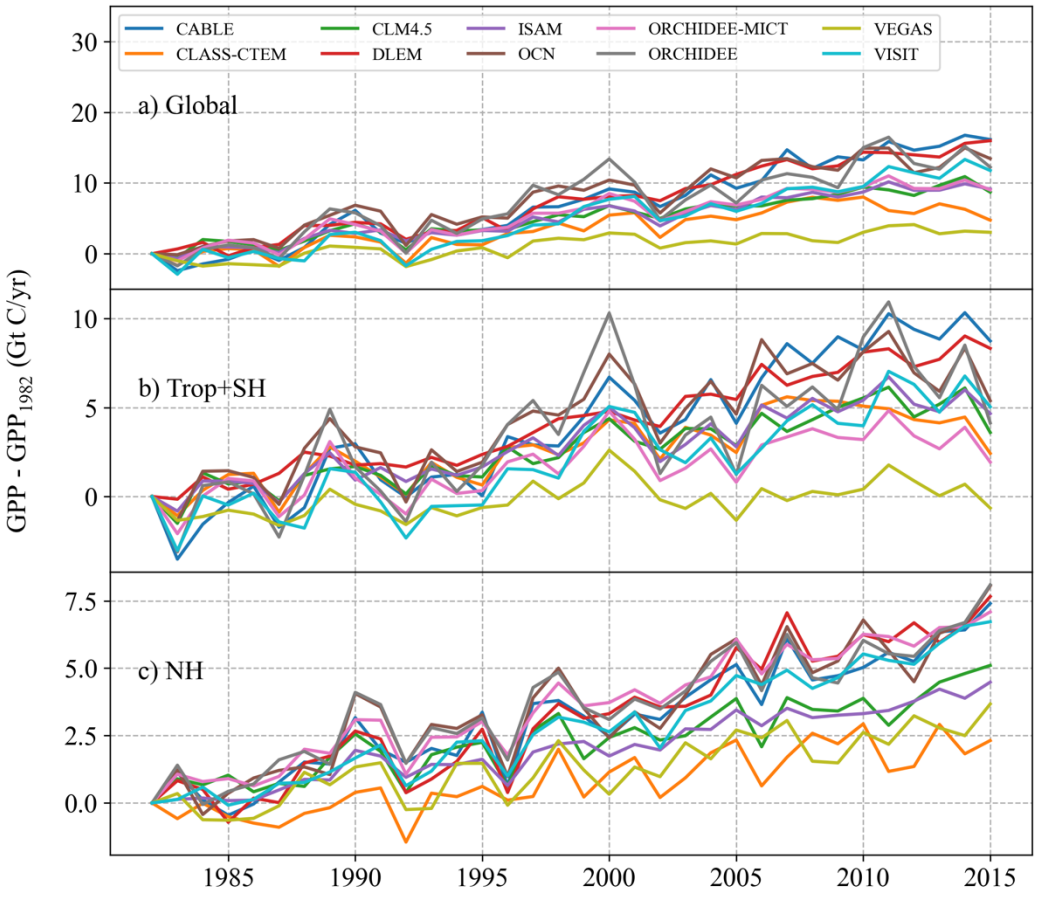

Figure S5: Changes of annual total GPP relative to 1982 for individual DGVM simulations.

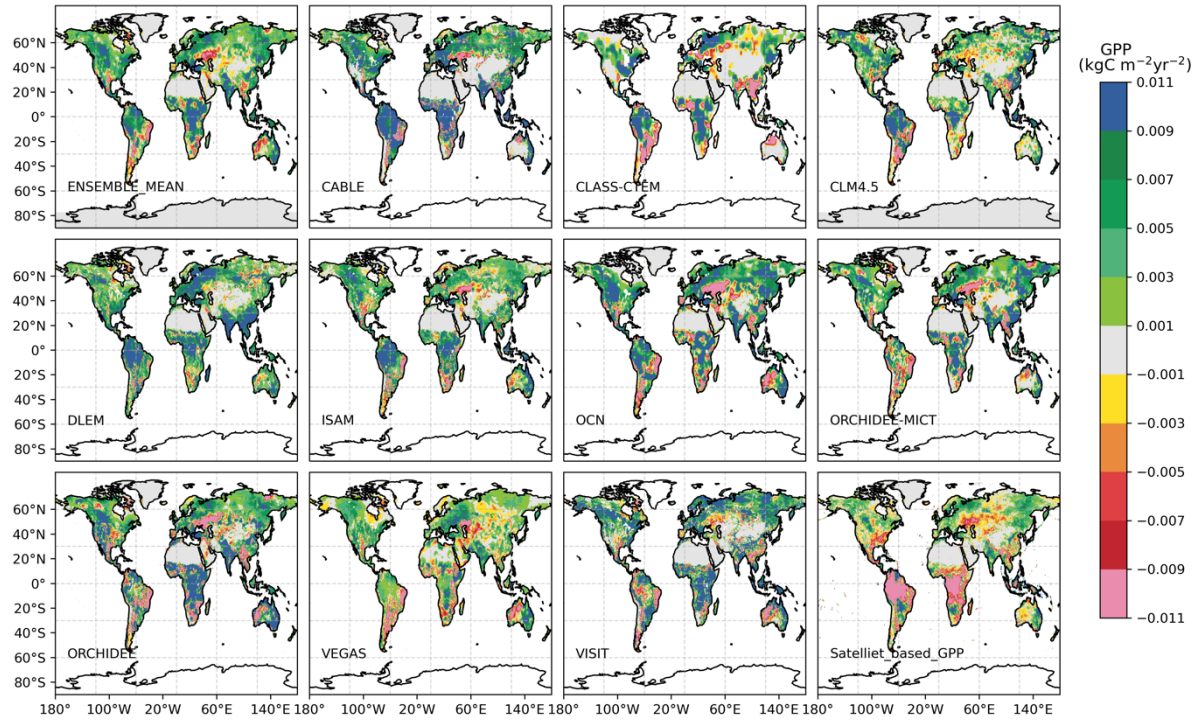

Figure S6: Geographical distributions of linear trends of GPP from satellite-based products and DGVM simulations (2001–2015). The unit of GPP trend is kgC m^{-2} yr^{-2}.

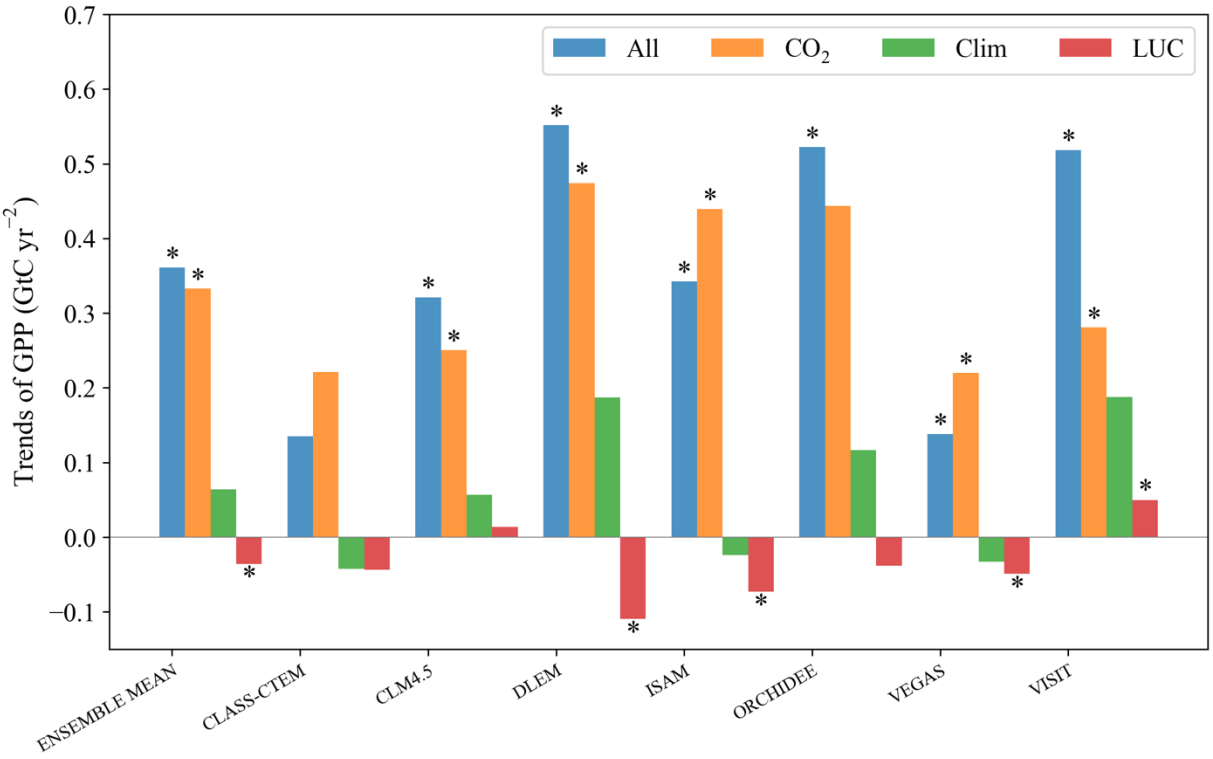

Figure S7: Attributions of global total GPP trends for TRENDYv6 simulations during 2001–2015: CO_2 fertilization effect (S1), climate (S2-S1), and land use change (S3-S2). "All" gives the values of the reference simulation that includes the effect of all three drivers (S3). Asterisks indicate that the trend is significant with $p < 0.05$ following the non-parametric Mann-Kendall trend test.

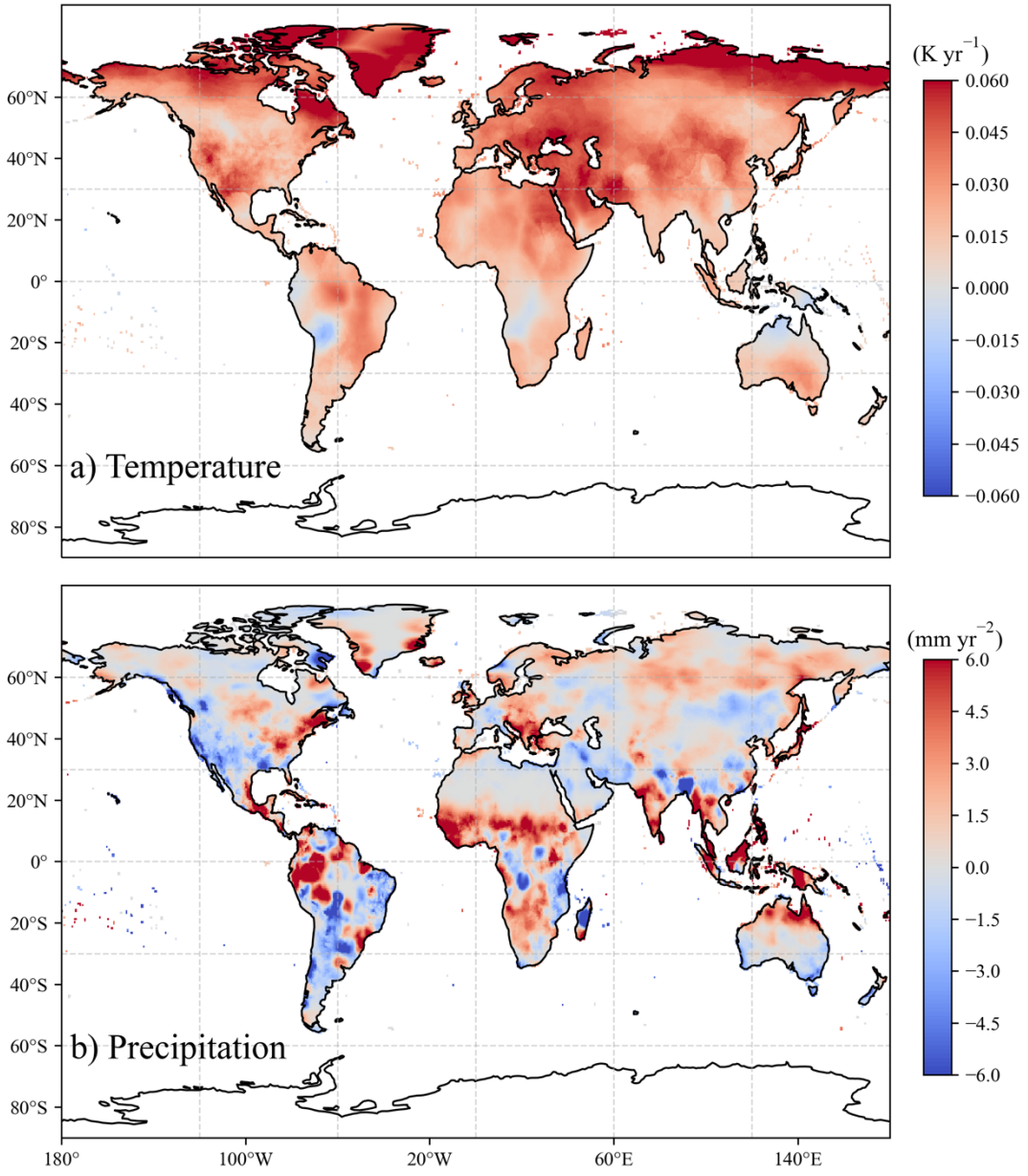

Figure S8: Geographical distributions of linear trends of (a) temperature and (b) precipitation from CRU datasets during 1982 to 2015. The trends of temperature and precipitation are K/yr^{-1} and mm/yr^{-2}, respectively.

85

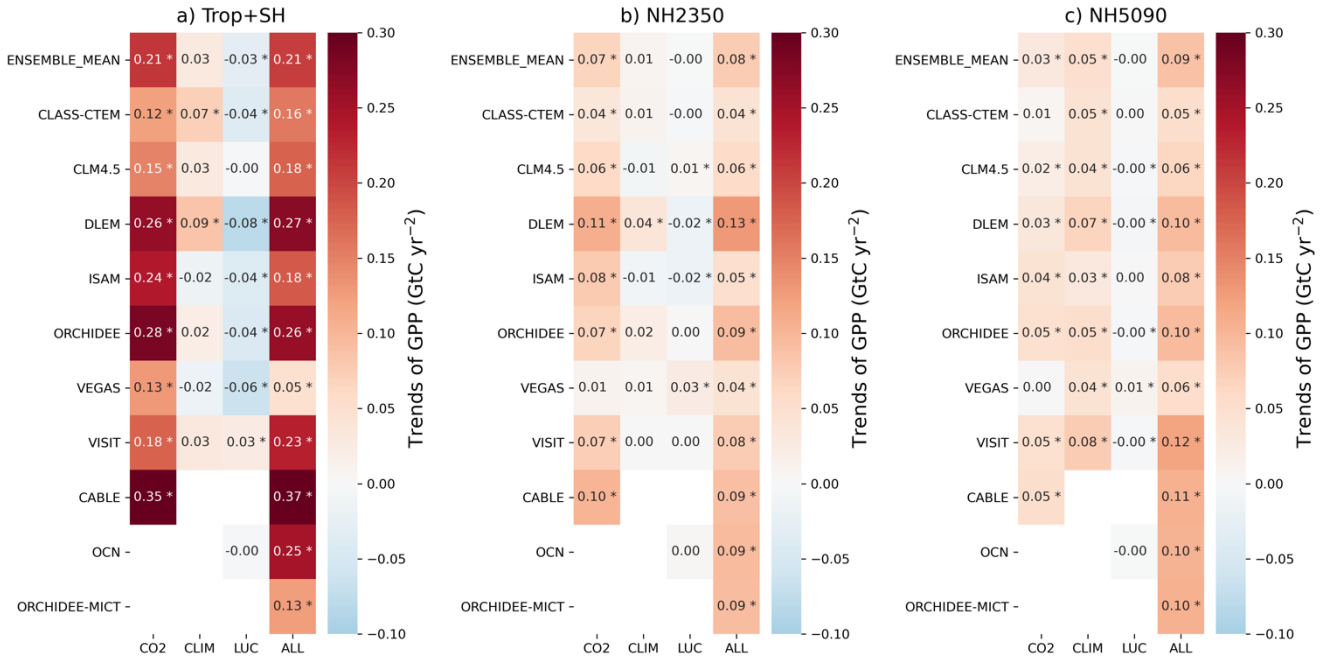

Figure S9: Regional GPP trends in individual model for the period of 1982–2015. CO_2 fertilization effect (S1), climate (S2-S1), LUC (S3-S2). "All" gives the values of the reference simulation that includes the effect of all three drivers (S3). NH2350 and NH5909 mean 50°N–90°N and 23°N–90°N, respectively. Asterisks indicate that the trend is significant with $p < 0.05$ following the non-parametric Mann-Kendall trend test.

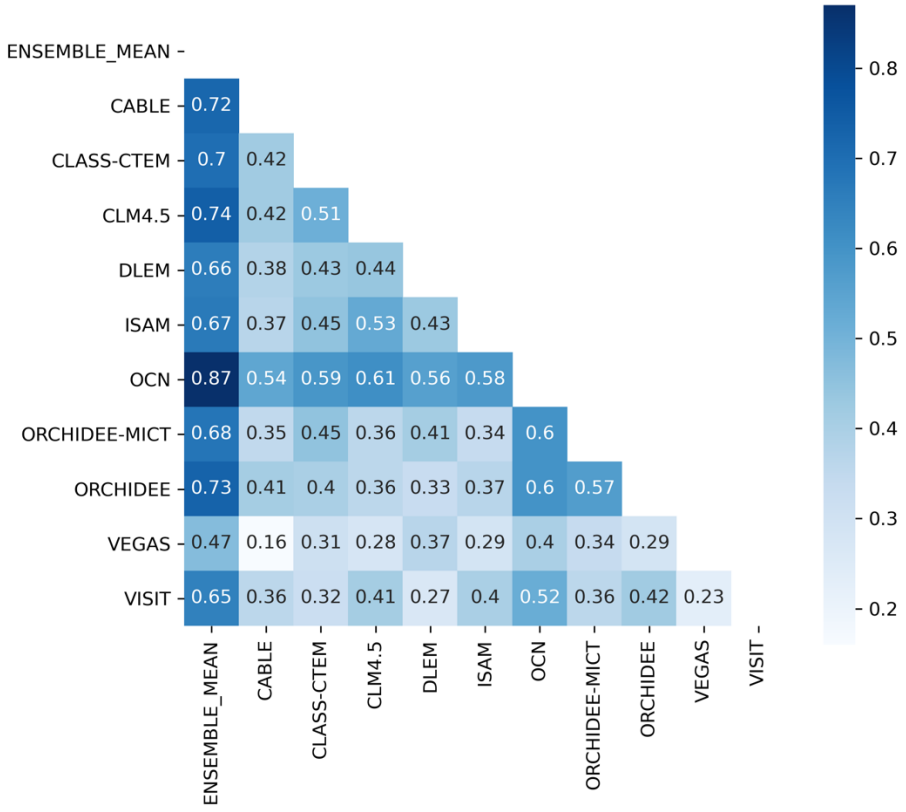

Figure S10: Spatial correlation coefficients among DGVM simulated GPP trends in pairs during 1982–2015.

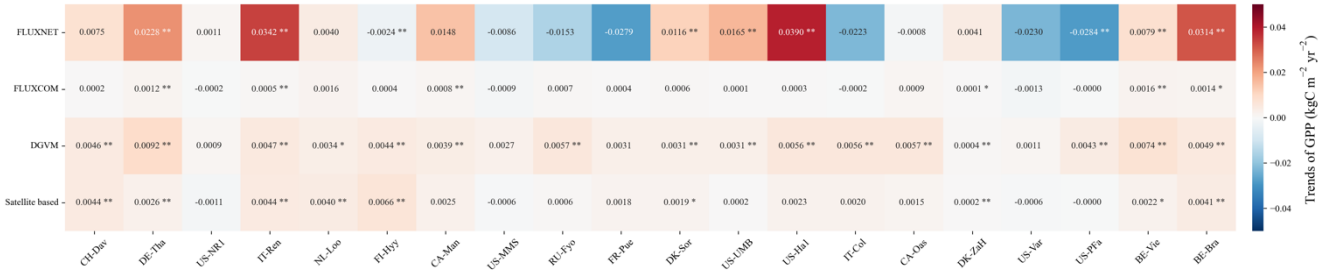

Figure S11: Trends of GPP at sites. The global GPP datasets were interpolated into the locations of these sites according to the bilinear interpolation method. The unit of GPP trend is kgC m $^{-2}$ yr^{-2}.

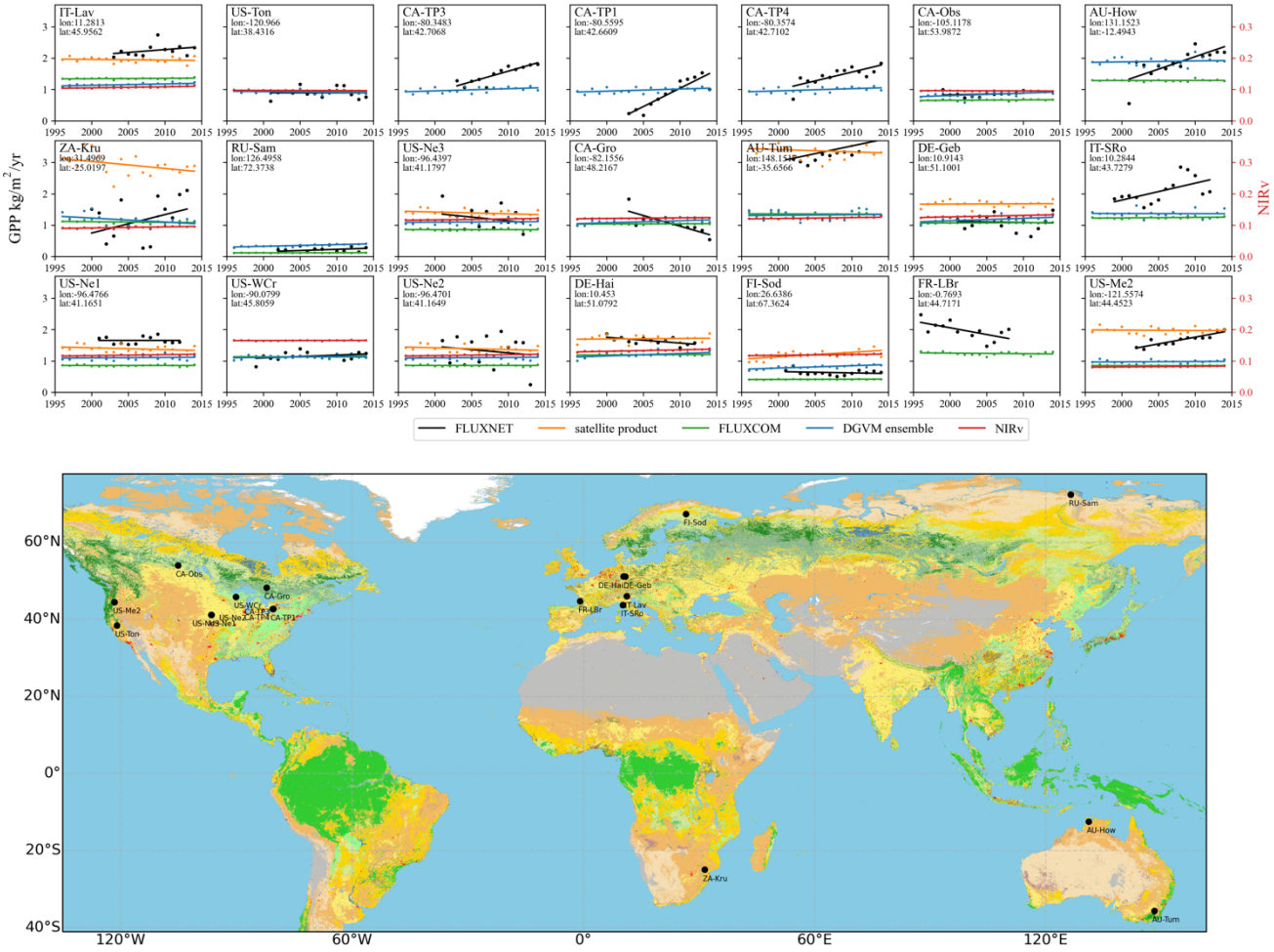

Figure S12: Comparisons of annual GPP over different FLUXNET2015 sites (black), FLUXCOM (green), satellite-based product (orange), DGVM ensemble (blue), and NIRv (red). The global GPP datasets were interpolated into the locations of these 21 sites according to the bilinear interpolation method. Observation sites with significant trends are marked with values. Single (*) and double (**) asterisks indicate that the trend is significant with $p < 0.1$ and $p < 0.05$ following the non-parametric Mann-Kendall trend test. The units of GPP and GPP trend are kgC m^{-2} yr^{-1} and kgC m^{-2} yr^{-2} respectively.

References

Harris, I., Jones, P. D., Osborn, T. J., and Lister, D. H.: Updated high-resolution grids of monthly climatic observations - the CRU TS3.10 Dataset, International Journal of Climatology, 34, 623-642, 10.1002/joc.3711, 2014.

Jung, M., Schwalm, C., Migliavacca, M., Walther, S., Camps-Valls, G., Koirala, S., Anthoni, P., Besnard, S., Bodesheim, P., Carvalhais, N., Chevallier, F., Gans, F., Goll, D. S., Haverd, V., Köhler, P., Ichii, K., Jain, A. K., Liu, J., Lombardozzi, D., Nabel, J. E. M. S., Nelson, J. A., O'Sullivan, M., Pallandt, M., Papale, D., Peters, W., Pongratz, J., Rödenbeck, C., Sitch, S., Tramontana, G., Walker, A., Weber, U., and Reichstein, M.: Scaling carbon fluxes from eddy covariance sites to globe:

synthesis and evaluation of the FLUXCOM approach, Biogeosciences, 17, 1343-1365, 10.5194/bg-17-1343-2020, 2020.

Pastorello, G., Trotta, C., Canfora, E., Chu, H., Christianson, D., Cheah, Y.-W., Poindexter, C., Chen, J., Elbashandy, A., Humphrey, M., Isaac, P., Polidori, D., Ribeca, A., van Ingen, C., Zhang, L., Amiro, B., Ammann, C., Arain, M. A., Ardo, J., Arkebauer, T., Arndt, S. K., Arriga, N., Aubinet, M., Aurela, M., Baldocchi, D., Barr, A., Beamesderfer, E., Marchesini, L. B., Bergeron, O., Beringer, J., Bernhofer, C., Berveiller, D., Billesbach, D., Black, T. A., Blanken, P. D., Bohrer, G., Boike, J., Bolstad, P. V., Bonal, D., Bonnefond, J.-M., Bowling, D. R., Bracho, R., Brodeur, J., Bruemmer, C., Buchmann, N., Burban, B., Burns, S. P., Buysse, P., Cale, P., Cavagna, M., Cellier, P., Chen, S., Chini, I., Christensen, T. R., Cleverly, J., Collalti, A., Consalvo, C., Cook, B. D., Cook, D., Coursolle, C., Cremonese, E., Curtis, P. S., D'Andrea, E., da Rocha, H., Dai, X., Davis, K. J., De Cinti, B., de Grandcourt, A., De Ligne, A., De Oliveira, R. C., Delpierre, N., Desai, A. R., Di Bella, C. M., di Tommasi, P., Dolman, H., Domingo, F., Dong, G., Dore, S., Duce, P., Dufrene, E., Dunn, A., Dusek, J., Eamus, D., Eichelmann, U., ElKhidir, H. A. M., Eugster, W., Ewenz, C. M., Ewers, B., Famulari, D., Fares, S., Feigenwinter, I., Feitz, A., Fensholt, R., Filippa, G., Fischer, M., Frank, J., Galvagno, M., Gharun, M., Gianelle, D., Gielen, B., Gioli, B., Gitelson, A., Goded, I., Goeckede, M., Goldstein, A. H., Gough, C. M., Goulden, M. L., Graf, A., Griebel, A., Gruening, C., Gruenwald, T., Hammerle, A., Han, S., Han, X., Hansen, B. U., Hanson, C., Hatakka, J., He, Y., Hehn, M., Heinesch, B., Hinko-Najera, N., Hoertnagl, L., Hutley, L., Ibrom, A., Ikawa, H., Jackowicz-Korczynski, M., Janous, D., Jans, W., Jassal, R., Jiang, S., Kato, T., Khomik, M., Klatt, J., Knohl, A., Knox, S., Kobayashi, H., Koerber, G., Kolle, O., Kosugi, Y., Kotani, A., Kowalski, A., Kruijt, B., Kurbatova, J., Kutsch, W. L., Kwon, H., Launiainen, S., Laurila, T., Law, B., Leuning, R., Li, Y., Liddell, M., Limousin, J.-M., Lion, M., Liska, A. J., Lohila, A., Lopez-Ballesteros, A., Lopez-Blanco, E., Loubet, B., Loustau, D., Lucas-Moffat, A., Lueers, J., Ma, S., Macfarlane, C., Magliulo, V., Maier, R., Mammarella, I., Manca, G., Marcolla, B., Margolis, H. A., Marras, S., Massman, W., Mastepanov, M., Matamala, R., Matthes, J. H., Mazzenga, F., McCaughey, H., McHugh, I., McMillan, A. M. S., Merbold, L., Meyer, W., Meyers, T., Miller, S. D., Minerbi, S., Moderow, U., Monson, R. K., Montagnani, L., Moore, C. E., Moors, E., Moreaux, V., Moureaux, C., Munger, J. W., Nakai, T., Neirynck, J., Nesic, Z., Nicolini, G., Noormets, A., Northwood, M., Nosetto, M., Nouvellon, Y., Novick, K., Oechel, W., Olesen, J. E., Ourcival, J.-M., Papuga, S. A., Parmentier, F.-J., Paul-Limoges, E., Pavelka, M., Peichl, M., Pendall, E., Phillips, R. P., Pilegaard, K., Pirk, N., Posse, G., Powell, T., Prasse, H., Prober, S. M., Rambal, S., Rannik, U., Raz-Yaseef, N., Reed, D., de Dios, V. R., Restrepo-Coupe, N., Reverter, B. R., Roland, M., Sabbatini, S., Sachs, T., Saleska, S. R., Sanchez-Canete, E. P., Sanchez-Mejia, Z. M., Schmid, H. P., Schmidt, M., Schneider, K., Schrader, F., Schroder, I., Scott, R. L., Sedlak, P., Serrano-Ortiz, P., Shao, C., Shi, P., Shironya, I., Siebicke, L., Sigut, L., Silberstein, R., Sirca, C., Spano, D., Steinbrecher, R., Stevens, R. M., Sturtevant, C., Suyker, A., Tagesson, T., Takanashi, S., Tang, Y., Tapper, N., Thom, J., Tiedemann, F., Tomassucci, M., Tuovinen, J.-P., Urbanski, S., Valentini, R., van der Molen, M., van Gorsel, E., van Huissteden, K., Varlagin, A., Verfaillie, J., Vesala, T., Vincke, C., Vitale, D., Vygodskaya, N., Walker, J. P., Walter-Shea, E., Wang, H., Weber, R., Westermann, S., Wille, C., Wofsy, S., Wohlfahrt, G., Wolf, S., Woodgate, W., Li, Y., Zampedri, R., Zhang, J., Zhou, G., Zona, D., Agarwal, D., Biraud, S., Torn, M., and Papale, D.: The FLUXNET2015 dataset and the ONEFlux processing pipeline for eddy covariance data, Scientific Data, 7, 10.1038/s41597-020-0534-3, 2020.

Sitch, S., Friedlingstein, P., Gruber, N., Jones, S. D., Murray-Tortarolo, G., Ahlström, A., Doney, S. C., Graven, H., Heinze, C., Huntingford, C., Levis, S., Levy, P. E., Lomas, M., Poulter, B., Viovy, N., Zaehle, S., Zeng, N., Arneth, A., Bonan, G., Bopp, L., Canadell, J. G., Chevallier, F., Ciais, P., Ellis, R., Gloor, M., Peylin, P., Piao, S. L., Le Quéré, C., Smith, B., Zhu, Z., and Myneni, R.: Recent trends and drivers of regional sources and sinks of carbon dioxide, Biogeosciences, 12, 653-679, 10.5194/bg-12-653-2015, 2015.

Wang, S., Zhang, Y., Ju, W., Chen, J. M., Ciais, P., Cescatti, A., Sardans, J., Janssens, I. A., Wu, M., Berry, J. A., Campbell, E., Fernandez-Martinez, M., Alkama, R., Sitch, S., Friedlingstein, P., Smith, W. K., Yuan, W., He, W., Lombardozzi, D., Kautz, M., Zhu, D., Lienert, S., Kato, E., Poulter, B., Sanders, T. G. M., Kruger, I., Wang, R., Zeng, N., Tian, H., Vuichard, N., Jain, A. K., Wiltshire, A., Haverd, V., Goll, D. S., and Penuelas, J.: Recent global decline of CO2 fertilization effects on vegetation photosynthesis, Science, 370, 1295–1300, https://doi.org/10.1126/science.abb7772, 2020

Xiao, Z., Liang, S., Wang, J., Xiang, Y., Zhao, X., and Song, J.: Long-Time-Series Global Land Surface Satellite Leaf Area Index Product Derived From MODIS and AVHRR Surface Reflectance, Ieee Transactions on Geoscience and Remote Sensing, 54, 5301-5318, 10.1109/tgrs.2016.2560522, 2016.

Yuan, W., Liu, S., Yu, G., Bonnefond, J.-M., Chen, J., Davis, K., Desai, A. R., Goldstein, A. H., Gianelle, D., Rossi, F., Suyker, A. E., and Verma, S. B.: Global estimates of evapotranspiration and gross primary production based on MODIS and global meteorology data, Remote Sensing of Environment, 114, 1416-1431, 10.1016/j.rse.2010.01.022, 2010.

Zheng, Y., Shen, R., Wang, Y., Li, X., Liu, S., Liang, S., Chen, J. M., Ju, W., Zhang, L., and Yuan, W.: Improved estimate of global gross primary production for reproducing its long-term variation, 1982-2017, Earth System Science Data, 12, 2725-2746, 10.5194/essd-12-2725-2020, 2020.